This article has been accepted for inclusion in a future issue of this journal. Content is final as presented, with the exception of pagination.

Trailer Steering Control of a Tractor–Trailer Robot

Paul Ritzen, Erik Roebroek, Nathan van de Wouw, Zhong-Ping Jiang, *Fellow, IEEE*, and Henk Nijmeijer, *Fellow, IEEE*

***Abstract*— In this paper, we consider active trailer steering control as a means to improve the maneuverability of (long) truck–trailer combinations during cornering. Hereto, we formulate the problem of reducing the so-called swept path width during cornering and that of eliminating unsafe tail swing of the trailer as a tracking control problem. We present a kinematic tractor–trailer model including off-axle hitching, on the basis of which we design nonlinear control strategies solving this tracking problem. The effectiveness of the proposed approach is evidenced experimentally on a robotic tractor–trailer platform.**

***Index Terms*— Active trailer steering, kinematics, nonlinear control, path following, tracking control, tractor–trailer robot.**

I. INTRODUCTION

LONG COMBINATION truck–trailer vehicles are gradually becoming more common in certain countries (Australia, USA, Scandinavian countries) because of advantages related to reduced costs for goods transportation and reduced fuel consumption (i.e., reduced impact on the environment). However, drawbacks related to inferior vehicle maneuverability hamper widespread introduction of such vehicles in Europe. In particular, the space required by a (conventional) tractor–trailer combination during a turning maneuver, the so-called swept path, is an important maneuverability/safety aspect [1]. Especially in urban areas or on narrow roads, the available space is limited and turning a maneuver, such as taking a 90° turn or taking a roundabout, can be a difficult and even an unsafe task, especially for long combination (truck–trailer) vehicles.

A solution to reduce the swept path width of a tractor–trailer combination is found in the application of trailer axle steering, as evidenced by existing trailer steering systems on the market [2], [3]. Although these systems reduce the swept path width, a further reduction in swept path width can be obtained using more advanced control strategies for trailer axle steering. Furthermore, these systems generate tail swing during transient cornering, i.e., during entering and exiting a turn, which represents a serious safety hazard.

Let us discuss the existing literature on active trailer steering control by subsequently addressing the following aspects: 1) the model type employed; 2) the particular control problem considered; and 3) the control strategy proposed. In this paper, we focus on active trailer steering for the improvement of low-speed maneuverability of tractor–trailer systems, not on its application toward improving lateral stability at high speeds.

In recent works on trailer steering control [4]–[8], a tractor–trailer vehicle with trailer steering is modeled *kinematically*, in which a nonholonomic velocity constraint is used to ideally model the absence of lateral tire slipping. Especially during low-speed maneuvers, such kinematic models can be considered to be accurate since inertial effects can then be neglected (provided that tire slip effects are indeed negligible). In [5] and [9]–[16], a linearized *dynamic* model is used to model an articulated vehicle, while [17]–[19] use a nonlinear dynamic model. In this way, dynamic effects can be evaluated, which significantly affect the behavior of the vehicle, although mainly during high speeds. Furthermore, in [4]–[6], [9]–[15], [18], and [19], off-axle hitching is included in the model, while [4] and [7] consider on-axle hitching. Especially during sharp turning maneuvers, the presence of off-axle hitching significantly affects the behavior of the tractor–trailer combination and hence should be included in the model description. Since this paper aims to improve *low-speed* maneuverability by axle steering control with validation on an (experimental) tractor–trailer *robotic* platform, in which tire slipping effects are indeed negligible, we pursue a kinematic modeling approach including off-axle hitching. In the applications of trail steering control in vehicular (heavy-duty) systems, effects regarding tire slipping may be important even at lower speeds.

Different control problem formulations for active trailer steering have been considered in [20]. In [7], [9], [10], [13], [18], and [21], the steering angle(s) of (multiple) *tractor* axle(s) is considered as a control input(s) and a reference path for the front tractor axle is prescribed. Such a control problem formulation would require fully automated vehicles in order to achieve path following. The problem considered in this paper is that of active *trailer* steering control for truck–trailer combinations in which a *human driver* determines the path (and speed) driven by the tractor (see also [6], [11], [14], [17], [19], [22]). In this setting, we consider: 1) the trailer axle steering speed as the control input and 2) the problem

Manuscript received January 16, 2015; revised September 17, 2015; accepted October 17, 2015. Manuscript received in final form November 3, 2015. This work was supported by the National Science Foundation under Grant ECCS-1230040. Recommended by Associate Editor A. Serrani.

P. Ritzen, E. Roebroek, and H. Nijmeijer are with the Department of Mechanical Engineering, Eindhoven University of Technology, Eindhoven 5600 MB, The Netherlands (e-mail: paul.ritzen@gmail.com; roebroek.erik@gmail.com; h.nijmeijer@tue.nl).

N. van de Wouw is with the the Department of Mechanical Engineering, Eindhoven University of Technology, Eindhoven 5600 MB, The Netherlands, also with the Department of Civil, Environmental and Geo-Engineering, University of Minnesota, Minneapolis, MN 55455 USA, and also with the Delft Center for Systems and Control, Delft University of Technology, Delft 2628 CD, The Netherlands (e-mail: n.v.d.wouw@tue.nl).

Z.-P. Jiang is with the Department of Electrical and Computer Engineering, Polytechnic School of Engineering, New York University, Brooklyn, NY 11201 USA (e-mail: zjiang@nyu.edu).

Color versions of one or more of the figures in this paper are available online at http://ieeexplore.ieee.org.

Digital Object Identifier 10.1109/TCST.2015.2499699

of reducing the swept path width (and tail swing) by ensuring that the trailer axle (or the trailer tail) follows the path of the tractor front axle.

In the literature, a range of different control strategies for trailer steering control have been proposed: an adaptive approach in [9] and [13], an H_∞ approach in [10], linear quadratic regulator control in [11], classical linear control in [6] and [14], a fuzzy control approach in [17], a Lyapunov-based approach in [7], and an approach based on backstepping in [18]. In these papers, the considered problems are formulated as a path-following problem, while in this paper, the path-following problem is reformulated as a tracking problem, for which subsequently nonlinear controllers based on feedback linearization and backstepping techniques are designed.

The main contributions of this paper are as follows. First, we reformulate the problem of reducing the swept path width and avoiding tail swing as a tracking problem for a kinematic (reference) model of the tractor–trailer system including off-axle hitching. We note that most of the work on the control of robotic tractor–trailer systems has focused on path-following problems where the tractor needs to follow a certain path [23]–[26], while here we focus on ensuring path following by the trailer of path driver by the tractor in order to support the minimization of the swept path width while avoiding tail swing. The latter problem is highly relevant in the control of trailers of heavy-duty vehicles [6], [10], [11] and the reformulation of the problem into a tracking problem for the variables describing the kinematics of the trailer supports the design of nonlinear controllers formally guaranteeing the stabilization of the desired trajectory. Second, nonlinear controllers solving this tracking problem are proposed, including stability certificates. Third, the experimental validation of the proposed control strategies on a newly developed *robotic* tractor trailer platform illustrates the effectiveness of the proposed control strategy.

The remainder of this paper is organized as follows. In Section II, we derive the kinematic tractor–trailer model. In Section III, the control problem is formulated in detail. In Section IV, we propose our controller design scheme, solving this problem, and present related stability results. In Section V, a simulation study is presented to evidence the effectiveness of the proposed approach and to support controller gain tuning. The control strategy will be further validated experimentally in Section VI. Finally, in Section VII, we present conclusions.

II. Model of the Tractor–Trailer Robot

In this section, a kinematic model is derived for the off-axle tractor–trailer robot, as shown in Fig. 1. We aim to construct a state-space model formulation such that the front wheel steering angle and its forward velocity are given time-varying (driver) inputs and the trailer axle steering velocity is the (only) control input. Hence, in this formulation, the tractor of the robot is steered and driven by an (emulated) *driver* and the trailer axle is steered automatically, improving maneuverability.

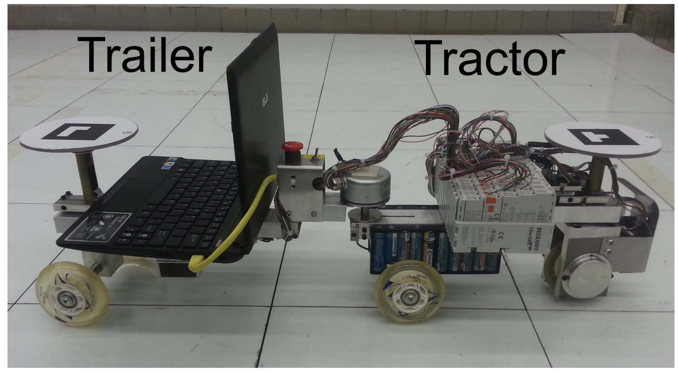

Fig. 1. Tractor–trailer robot. The right side of the robot is the tractor with a steered and driven front wheel. The left side of the robot is the trailer with a steered trailer axle. The trailer articulates at the hitch point that connects the trailer to the tractor. The tractor front wheel steering angle, the trailer axle steering angle, and the articulation angle are measured.

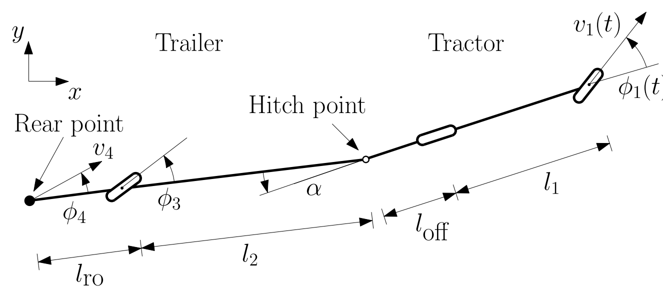

Fig. 2. Bicycle-like schematic model representation of the tractor–trailer robot.

As we consider low-speed turning maneuvers in this paper, and given the fact that the robot has single rear axles both at the tractor and trailer, the assumption of no sideways slip (between the wheels and the floor) is justified. Consequently, a kinematic model can accurately describe the behavior of the tractor–trailer robot and further dynamic effects, related to wheel slip and inertial effects, can be neglected.

Consider a bicycle-like model representation as shown in Fig. 2. Each wheel in Fig. 2 represents the midpoint of an axle (from right to left: the tractor front axle, the tractor rear axle, and the trailer axle). Furthermore, the trailer rear point (tail) and the articulation (hitch) point between the tractor and trailer are illustrated as well. The lengths characterizing the tractor, trailer, and axle locations are defined as follows: the tractor body length l_1, the off-axle distance l_{off}, the trailer length l_2, and the rear overhang l_{ro}. The front wheel steering angle ϕ_1 and forward velocity v_1, as well as the articulation angle α and the trailer wheel steering angle ϕ_3 are shown in Fig. 2. In addition, the relative heading angle ϕ_4 of the trailer rear point (tail) is illustrated, which characterizes the direction of the velocity v_4 of the trailer rear point.

The driver input $\mathbf{d}(t) := [v_1(t), \phi_1(t)]$ consists of the forward velocity $v_1(t)$ and the steering angle $\phi_1(t)$ of the tractor front wheel, which are both considered to be given and to depend explicitly on time.

The fixed-world posture of the tractor with respect to the frame (x, y) can be characterized by the coordinates $(\theta_1, \delta_1, X_1, Y_1)$, see Fig. 3. This posture is completely

This article has been accepted for inclusion in a future issue of this journal. Content is final as presented, with the exception of pagination.

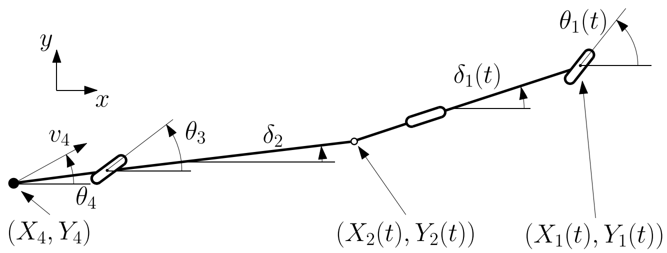

Fig. 3. Tractor–trailer posture in fixed-world coordinates.

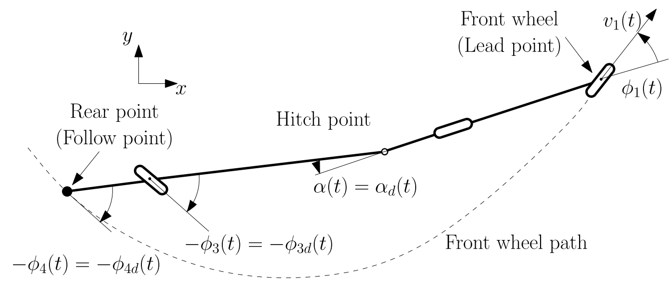

Fig. 4. Reference trailer configuration.

determined by the driver input $\mathbf{d}(t)$ (and the initial posture of the tractor) and, therefore, can also be considered as a given function of time:

$$\begin{aligned} \theta_1(t) &= \phi_1(t) + \frac{1}{l_1}\int_0^t v_1(\sigma)\sin\phi_1(\sigma)d\sigma \\ \delta_1(t) &= \frac{1}{l_1}\int_0^t v_1(\sigma)\sin\phi_1(\sigma)d\sigma \\ X_1(t) &= \int_0^t v_1(\sigma)\cos\theta_1(\sigma)d\sigma \\ Y_1(t) &= \int_0^t v_1(\sigma)\sin\theta_1(\sigma)d\sigma. \end{aligned} \tag{1}$$

Herein, we presume, without loss of generality, that $\theta_1(t_0) = \phi_1(t_0) = X_1(t_0) = Y_1(t_0) = 0$ with $t_0 = 0$. These initial conditions imply that the robot is initially aligned with the x-axis and the tractor front wheel is located at the origin. The location $(X_2(t), Y_2(t))$ of the hitch point can be expressed as a given function of time as well

$$\begin{aligned} X_2(t) &= X_1(t) - (l_1 + l_{\text{off}})\cos\delta_1(t) \\ Y_2(t) &= Y_1(t) - (l_1 + l_{\text{off}})\sin\delta_1(t). \end{aligned} \tag{2}$$

Note that, effectively, the motion of the entire tractor is given as a function of time (determined by the driver input).

The articulation angle α is equal to the difference between the orientation of the tractor body $\delta_1(t)$ and that of the trailer body δ_2

$$\alpha = \delta_1(t) - \delta_2. \tag{3}$$

Using angular kinematics, the rotational velocity $\dot{\delta}_2$ of the trailer body can be expressed as

$$\dot{\delta}_2 = \frac{1}{l_2}c_2(t)c_3(\mathbf{x}) - \frac{l_{\text{off}}}{l_1 l_2}c_1(t)c_4(\mathbf{x}), \tag{4}$$

in which

$$\begin{aligned} c_1(t) &:= v_1(t)\sin\phi_1(t) \\ c_2(t) &:= v_1(t)\cos\phi_1(t) \\ c_3(\mathbf{x}) &:= \sin\alpha - \cos\alpha\tan\phi_3 \\ c_4(\mathbf{x}) &:= \cos\alpha + \sin\alpha\tan\phi_3 \end{aligned} \tag{5}$$

for $\phi_3 \in (-(\pi/2), (\pi/2))$, and where $\mathbf{x} := [\alpha \;\; \phi_3]^T$. Then, we can express the position of the rear point of the trailer, characterized by coordinates (X_4, Y_4), as

$$\begin{aligned} X_4 &= X_1(t) - (l_1 + l_{\text{off}})\cos\delta_1(t) - (l_2 + l_{\text{ro}})\cos\delta_2 \\ Y_4 &= Y_1(t) - (l_1 + l_{\text{off}})\sin\delta_1(t) - (l_2 + l_{\text{ro}})\sin\delta_2. \end{aligned} \tag{6}$$

Furthermore, the heading angles θ_3 and θ_4 of the trailer wheel and the rear point are, respectively, given by

$$\theta_3 = \delta_2 + \phi_3 \tag{7}$$

$$\theta_4 = \delta_2 + \phi_4. \tag{8}$$

Using the kinematic relations derived in (1)–(4), the trailer dynamics can be expressed in terms of the state $\mathbf{x} = [\alpha \;\; \phi_3]^T$ and can be written in a nonlinear and time-varying state-space form

$$\dot{\mathbf{x}} = \mathbf{f}(\mathbf{x}, \mathbf{d}(t)) + \mathbf{g}u \tag{9}$$

with the control input $u = \dot{\phi}_3$ and

$$\mathbf{f}(\mathbf{x}, \mathbf{d}(t)) := \begin{bmatrix} f_\alpha(\mathbf{x}, \mathbf{d}(t)) \\ 0 \end{bmatrix}, \quad \mathbf{g} := \begin{bmatrix} 0 \\ 1 \end{bmatrix}. \tag{10}$$

Herein

$$f_\alpha(\mathbf{x}, \mathbf{d}(t)) := \frac{1}{l_1}c_1(t) - \frac{1}{l_2}c_2(t)c_3(\mathbf{x}) + \frac{l_{\text{off}}}{l_1 l_2}c_1(t)c_4(\mathbf{x}) \tag{11}$$

with $c_1(t)$, $c_2(t)$, $c_3(\mathbf{x})$, and $c_4(\mathbf{x})$ as in (5).

The state-space model (5), (9)–(11) shows that the only control input u is the trailer wheel steering velocity $\dot{\phi}_3$ and the driver input $\mathbf{d}(t)$ is considered to be an *a priori* unknown function of time.

III. Control Problem Formulation

The main control goal considered in this paper is to reduce the swept path width of the tractor–trailer robot while avoiding tail swing. The latter objective can be achieved by ensuring that the rear point of the trailer follows the path driven by the front wheel of the tractor [8], [27]. Hence, in this section, we consider a path-following problem in which a follow point (rear point of the trailer) is required to follow the path driven by a lead point (front wheel of the tractor), see Fig. 4. This path-following problem, described in the x–y plane, is reformulated into a state tracking problem, described in terms of the state (α, ϕ_3).

A schematic of the resulting tracking control problem is shown in Fig. 5. The driver inputs $(\phi_1(t), v_1(t))$ are considered to be given (although not *a priori* known) and are used to construct the reference trailer kinematics, i.e., the desired state trajectory $(\alpha_d(t), \phi_{3d}(t))$. Furthermore, the behavior of the tractor–trailer robot is affected by the driver inputs and the control input u, which is the trailer wheel steering velocity, see the model in (9)–(11). In Section IV, we will propose

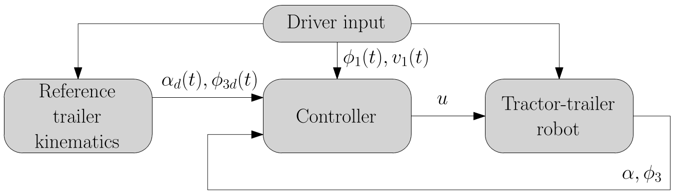

Fig. 5. Control block diagram.

control strategies to design controllers using the information on the measured state (articulation angle and trailer steering angle), the driver input, and the reference trailer kinematics.

Section III-A concerns the derivation of the reference trailer kinematics (i.e., the desired state variables $\alpha_d(t), \phi_{3d}(t)$ and their time derivatives) in order to reformulate the path-following problem into a state tracking problem. In Section III-B, we formulate assumptions amongst others needed to avoid singularities in the description of the reference trailer kinematics.

A. Reference Trailer Kinematics

The reference trailer kinematics describe the kinematics of the trailer for which it holds that the rear point of the trailer exactly follows the path driven by the tractor front wheel, also during transient cornering (see Fig. 4). Hence, these kinematics can be employed to generate the state reference trajectory $(\alpha_d(t), \phi_{3d}(t))$ for the control strategy presented in Section IV (in addition, time derivatives of $\alpha_d(t)$ and $\phi_{3d}(t)$ will be computed as well, because these are also needed in this control strategy).

To construct the reference kinematics in terms of $(\alpha_d(t), \phi_{3d}(t))$, we compute a feasible position for the rear point of the trailer on the path driven by the front wheel, given the length l_2 of the trailer and the rear overhang l_{ro}, by solving the following (minimization) problem:

$$\hat{\tau}(t) := \min_{\tau}\{\tau \geq 0 | f_\tau = 0\} \tag{12}$$

with

$$f_\tau := (X_2(t) - X_1(t-\tau))^2 + (Y_2(t) - Y_1(t-\tau))^2 - (l_2 + l_{\text{ro}})^2. \tag{13}$$

In this way, a feasible rear point trailer position on the driven tractor front wheel path can be found, i.e., which is located a distance of $l_2 + l_{\text{ro}}$ from the hitch point $(X_2(t), Y_2(t))$ (hence the form of f_τ in (13)). The solution $\hat{\tau}$ of the problem in (12) and (13) is the corresponding time difference between the time instant t at which the tractor front wheel is at a certain position and the time instant $t - \hat{\tau}$ at which the (desired) trailer rear point is at the same position. During transient cornering, the time difference $\hat{\tau}(t)$ is indeed time varying.

Remark 1: In order to prevent nonuniqueness of the solution of (12) and (13), certain assumptions on the tractor front wheel path have to be satisfied. These assumptions will be made explicit in Section III-B. In addition, we assume that for $t \leq 0$, it holds that $v_1(t) = v_1(0)$ and $\phi_1(t) = \phi_1(0) = 0$, such that there always exists a solution of the (minimization) problem (12), (13) at $t = 0$.

Based on the detailed developments in Appendix A, the state reference trajectory $(\alpha_d(t), \phi_{3d}(t))$ is given below. In particular, $\alpha_d(t)$ is given by

$$\alpha_d(t) = \delta_1(t) - \delta_{2d}(t) \tag{14}$$

where

$$\delta_{2d}(t) = 2\arctan\left(\frac{\Delta Y}{\sqrt{\Delta X^2 + \Delta Y^2} + \Delta X}\right) \tag{15}$$

with

$$\begin{aligned} \Delta X &:= X_2(t) - X_{4d}(t) \\ \Delta Y &:= Y_2(t) - Y_{4d}(t) \end{aligned} \tag{16}$$

and

$$\begin{aligned} X_{4d}(t) &:= X_1(t - \hat{\tau}(t)) \\ Y_{4d}(t) &:= Y_1(t - \hat{\tau}(t)) \end{aligned} \tag{17}$$

denoting the reference trajectory of the tail of the trailer. Moreover, $\phi_{3d}(t)$ is given by

$$\phi_{3d}(t) = \arctan\left(\frac{w_3(t) - w_1(t)}{w_2(t)}\right) \tag{18}$$

with $w_2(t) \neq 0$ for all t. In (18), $w_1(t)$, $w_2(t)$, and $w_3(t)$ are given by

$$\begin{aligned} w_1(t) &:= \frac{1}{l_1}c_1(t) - \frac{1}{l_2}c_2(t)\sin\alpha_d(t) + \frac{l_{\text{off}}}{l_1 l_2}c_1(t)\cos\alpha_d(t) \\ w_2(t) &:= \frac{1}{l_2}c_2(t)\cos\alpha_d(t) + \frac{l_{\text{off}}}{l_1 l_2}c_1(t)\sin\alpha_d(t) \\ w_3(t) &:= \frac{1}{l_1}c_1(t) - \frac{1}{l_2+l_{\text{ro}}}c_2(t)c_{5d}(t) + \frac{l_{\text{off}}}{l_1(l_2+l_{\text{ro}})}c_1(t)c_{6d}(t) \end{aligned} \tag{19}$$

with

$$\begin{aligned} c_{5d}(t) &:= \sin\alpha_d(t) - \cos\alpha_d(t)\tan\phi_{4d}(t) \\ c_{6d}(t) &:= \cos\alpha_d(t) + \sin\alpha_d(t)\tan\phi_{4d}(t). \end{aligned} \tag{20}$$

The reference trailer kinematics are now completely described in terms of the reference state trajectory $(\alpha_d(t), \phi_{3d}(t))$ (and related time derivatives). Note that for the construction of these reference kinematics, only the information on the driver input $(v_1(t), \phi_1(t))$ and the geometries of the truck–trailers l_1, l_2, l_{off}, and l_{ro} is required.

This desired state trajectory can be employed in the controller designed in Section IV.

B. Assumptions

In this section, we adopt two types of assumptions: 1) assumptions needed to avoid singularities in the description of the reference trailer kinematics, which will ultimately also be needed to avoid singularities in the (real) trailer kinematics, and 2) assumptions guaranteeing that a (physically realizable) solution to the (minimization) problem in (12) and (13) exists.

Assumption 1: The reference kinematics satisfy the following conditions:

1) There exists an $\varepsilon_1 > 0$ such that $\phi_{id}(t) \in [\varepsilon_1 - (\pi/2), (\pi/2) - \varepsilon_1]$ for all t and for $i = 3, 4$.
2) There exists an $\varepsilon_2 > 0$ such that $w_2(t) \geq \varepsilon_2$ for all t.

Assumption 1.1 implies that the desired velocity of the trailer wheel and that of the trailer tail are not allowed to be perpendicular to the trailer body, which are reasonable assumptions in practice [8]. Assumption 1.2 implies that the (desired) longitudinal trailer velocity $l_2 w_2(t)$ (with $w_2(t)$ given in (48)) should be strictly positive, which is again a reasonable assumption in practice (as the current control strategy is designed for normal forward driving conditions and not for backward driving).

Assumption 2 is related to the path driven by the tractor front wheel and is adopted to avoid scenarios that are physically infeasible or in which no (or undesirable) solutions to the (minimization) problem in (12) and (13) exist.

Assumption 2: The path driven by the tractor front wheel satisfies the following conditions:

1) The curvature $\kappa_1(t)$ of the path driven by the tractor front wheel should satisfy $\kappa_1(t) < (1/l_2 + l_{\text{ro}})$ for all $t \geq 0$.
2) The tractor front wheel velocity should be strictly positive, i.e., $v_1(t) > 0$ for all $t \geq 0$.
3) The total length of the trailer has to be longer than the total length of the tractor, i.e., $l_2 + l_{\text{ro}} > l_1 + l_{\text{off}}$.

Assumption 2.1 is adopted to avoid amongst others a scenario in which a physically infeasible trajectory would result in the sense that the trailer body would collide with that of the tractor. Assumption 2.2 avoids a scenario in which $v_1(t)$ changes sign resulting in a nonsmooth tractor front wheel path, which is infeasible for the trailer.

Remark 2: Assumption 2.2 avoids singularities in the reference kinematics (see Appendix A) and in the proposed control law (see Section IV), for $v_1(t) = 0$. The singularity in the reference kinematics could easily be resolved by setting $\dot{\alpha}_d(t) = \dot{\phi}_{3d}(t) = 0$ when $v_1(t) = 0$. The singularity in the control law for $v_1(t)$ is fundamental in nature as when $v_1(t) = 0$, controllability is essentially lost due to the fact that f_α in (11) is zero for $v_1(t) = 0$. In other words, we cannot steer the trailer toward the desired trajectory when $v_1(t) = 0$. However, this does not pose a problem in practice as the control action could be zeroed for $v_1(t) = 0$ while accepting that no convergence to the desired trajectory is achieved when the tractor stands still and that such convergence will only be guaranteed when the tractor starts moving again with a sufficiently large positive velocity.

Assumption 2.3 avoids a geometric scenario in which: 1) the trailer is too short to be put back on the tractor front wheel path or 2) multiple feasible positions on the tractor front wheel path exist for the trailer wheel and the solution to the (minimization) problem would be an undesirable one (see Fig. 6 for a geometric scenario in which Assumption 2.3 is violated).

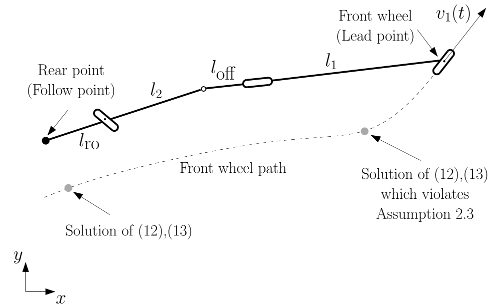

Fig. 6. Situation in which Assumption 2.3 is violated.

C. Discussion

Let us summarize the main conclusions from this section:

1) The path-following problem is conveniently reformulated as a reference state tracking problem in support of the controller design in Section IV.
2) The related state reference kinematics $(\alpha_d(t), \phi_{3d}(t))$ has been constructed.
3) Assumptions 1 and 2 are adopted, which are both reasonable assumptions in practice, first to avoid singularities in the description of the reference trailer kinematics, which will ultimately also be needed to avoid singularities in the (real) trailer kinematics, and second to guarantee that a (physically realizable) solution to the (minimization) problem in (12) and (13) exists.

Based on the formulation of the state tracking problem in Fig. 5, in the next section, we design a controller for the trailer wheel steering velocity u that exponentially stabilizes the desired trajectory $(\alpha_d(t), \phi_{3d}(t))$. In this way, the rear point exponentially tracks the reference trailer and hence follows the path driven by the tractor front wheel.

IV. Controller Design

In this section, a controller design will be proposed for the tractor–trailer robot, described by (5) and (9)–(11), which exponentially stabilizes the desired state trajectory $(\alpha_d(t), \phi_{3d}(t))$.[1] Since the desired trajectory $(\alpha_d(t), \phi_{3d}(t))$ may involve large angle trajectories (for realistic maneuvers such as 90° turn or driving part of a roundabout), a small-angle model approximation is inappropriate. Hence, we will propose a nonlinear controller design based on feedback linearization [30].

Consider the tractor–trailer dynamics in (5) and (9)–(11) and the reference trailer kinematics as described in Section III-A. We propose the following control law:

$$u = \zeta_2(\mathbf{x}, t)^{-1}(-\zeta_1(\mathbf{x}, t) + v) \tag{21}$$

with

$$\begin{aligned}
\zeta_1(\mathbf{x}, t) &= \zeta_{11}(\mathbf{x}, t) + \zeta_{12}(\mathbf{x}, t) + \zeta_{13}(\mathbf{x}, t) \\
\zeta_2(\mathbf{x}, t) &= \frac{c_2(t)\cos\alpha}{l_2\cos^2\phi_3} + \frac{c_1(t) l_{\text{off}}\sin\alpha}{l_1 l_2 \cos^2\phi_3} \\
v &= -k_1(\alpha - \alpha_d(t)) - k_2(\dot{\alpha} - \dot{\alpha}_d(t)),
\end{aligned} \tag{22}$$

[1] See [28] and [29] for background information on tracking control in generic nonlinear and mobile robotic contexts, respectively.

in which the controller gains $k_1, k_2 > 0$ and

$$\begin{aligned}\zeta_{11}(\mathbf{x}, t) &= c_7(t) - c_8(t)c_3(\mathbf{x}) + \frac{l_{\text{off}}}{l_2}c_7(t)c_4(\mathbf{x}) \\ \zeta_{12}(\mathbf{x}, t) &= -\frac{1}{l_2}c_2(t)c_4(\mathbf{x}) - \frac{l_{\text{off}}}{l_1 l_2}c_1(t)c_3(\mathbf{x}) \\ \zeta_{13}(\mathbf{x}, t) &= -\frac{c_2(t)\cos\alpha}{l_2\cos^2\phi_3} - \frac{c_1(t)l_{\text{off}}\sin\alpha}{l_1 l_2\cos^2\phi_3}\end{aligned} \tag{23}$$

with $c_1(t), c_2(t), c_3(\mathbf{x})$, and $c_4(\mathbf{x})$ as in (5) and

$$\begin{aligned}c_7(t) &:= \frac{1}{l_1}(\dot{v}_1(t)\sin(\phi_1(t)) + v_1(t)\dot{\phi}_1(t)\cos\phi_1(t)) \\ c_8(t) &:= \frac{1}{l_2}(\dot{v}_1(t)\cos\phi_1(t) - v_1(t)\dot{\phi}_1(t)\sin\phi_1(t)).\end{aligned} \tag{24}$$

In Theorem 1, it will be shown that this control law (locally) exponentially stabilizes the desired trajectory $(\alpha_d(t), \phi_{3d}(t))$ and, hence, solves the tracking problem formulated in Section III.

Theorem 1: Consider the tractor–trailer dynamics in (5) and (9)–(11) and the reference trailer kinematics in Section III-A. Adopt Assumptions 1 and 2 and consider the controller in (21)–(24). Then, the desired trajectory $(\alpha_d(t), \phi_{3d}(t))$ is a (locally) exponentially stable solution of the closed-loop system (5), (9)–(11), (21)–(24).

Proof: For the proof, see Appendix B. ■

Based on Theorem 1, we can conclude that the tracking problem posed in Section III is solved by the controller (21)–(24), implying that the trailer rear point indeed follows the path driven by the tractor front wheel.

Remark 3: Under Assumptions 1 and 2, an alternative control law (based on backstepping) that (locally) asymptotically stabilizes the desired trajectory $(\alpha_d(t), \phi_{3d}(t))$ can be designed as follows:

$$u = \beta_4^{-1}(-\beta_2 e_1 - \beta_3 - k_2 e_2) \tag{25}$$

with

$$\begin{aligned}e_1 &= \alpha - \alpha_d(t) \\ e_2 &= \tan\phi_3 + \beta_2^{-1}(\beta_1 + k_1 e_1) \\ \beta_1 &= \frac{1}{l_2}c_2(t)(c_3(t) - \sin\alpha) - \frac{l_{\text{off}}}{l_1 l_2}c_1(t)(c_4(t) - \cos\alpha) \\ \beta_2 &= \frac{1}{l_2}c_2(t)\cos\alpha + \frac{l_{\text{off}}}{l_1 l_2}c_1(t)\sin\alpha \\ \beta_3 &= \frac{d}{dt}\left(\beta_2^{-1}(\beta_1 + k_1 e_1)\right) \\ \beta_4 &= \frac{1}{\cos^2\phi_3},\end{aligned} \tag{26}$$

in which the controller gains $k_1, k_2 > 0$. A proof for the fact that this controller asymptotically stabilizes the desired trajectory $(\alpha_d(t), \phi_{3d}(t))$ can be obtained using backstepping results [28], [31] and is omitted here for the sake of brevity. For this control law, the singularities are similar to those of the control law given in Theorem 1 and can be avoided using similar arguments as those put forward in the proof of Theorem 1 for the controller (21)–(24).

TABLE I
DIMENSIONS OF THE TRACTOR–TRAILER ROBOT

Parameter	Value [m]
Tractor length l_1	0.209
Off-axle distance l_{off}	0.050
Trailer length l_2	0.312
Rear overhang l_{ro}	0.000

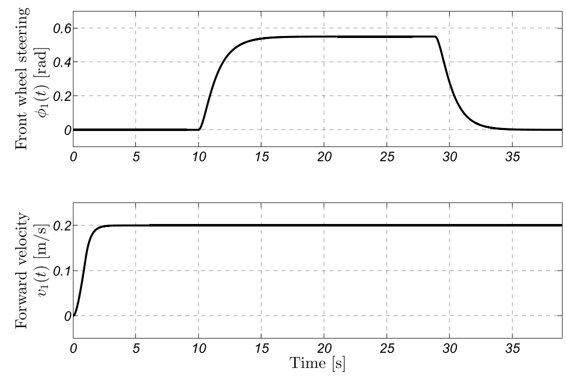

Fig. 7. Driver inputs for the 540° turning maneuver.

V. Simulation Results

To illustrate the effectiveness of the proposed control strategy, a simulation study of a 540° turning maneuver is performed in this section. The dimensions of the tractor–trailer robot in Fig. 1 are presented in Table I.

This section is organized as follows. In Section V-A, the 540° turning maneuver is described. In Section V-B, the controller gains are tuned based on the simulation results. Finally, the simulation results of the 540° turning maneuver are discussed in detail in Section V-C.

A. 540° Turning Maneuver

A 540° turning maneuver is considered both for the simulation study in this section and experimental study in Section VI. The maneuver consists of three phases:

1) driving a straight line section;
2) performing a 540° turn to the left with a tractor front wheel turning radius of $R = 0.4$ m;
3) driving a straight line section again.

During the transition between these phases, transient cornering occurs, i.e., $\dot{\phi}_3 \neq 0$ rad/s. Furthermore, in this type of maneuver, also steady-state cornering ($\dot{\phi}_3 = 0$ rad/s) can be observed. Therefore, this type of maneuver is representative of the cornering behavior observed in many other turning maneuvers, e.g., a 90° turn or a U-turn. In addition, we introduce an initial offset on the articulation angle: $\alpha(t = 0) = 0.3$ rad. Such an initialization allows us to observe and tune the transient convergence of the trailer rear point from $\alpha(t = 0) = 0.3$ rad toward $\alpha_d = 0$ rad (see Section V-B).

In Fig. 7, the driver inputs are plotted that ensure that the tractor front wheel performs the described 540° turning maneuver. Initially, the robot accelerates up to a forward velocity $v_1(t)$ of 0.2 m/s and maintains this velocity during the remainder of the maneuver. At $t = 10$ s, the front wheel

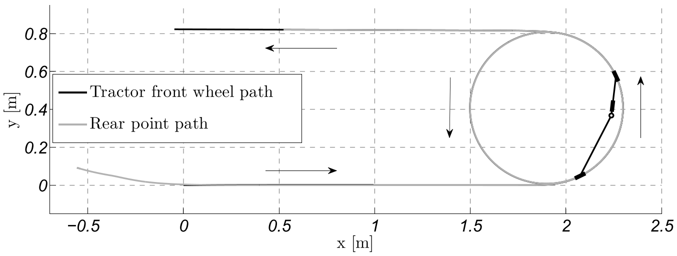

Fig. 8. Closed-loop tractor–trailer response for the controller (21)–(24).

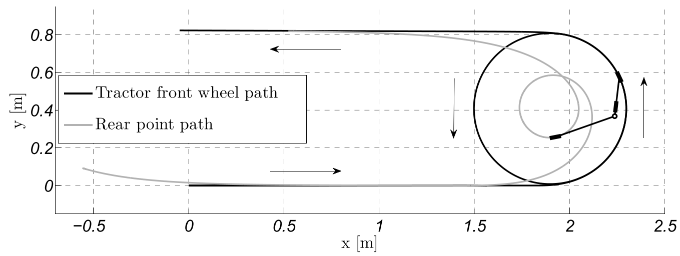

Fig. 9. Tractor–trailer response without trailer steering.

starts steering for $(3\pi R/v_1) = 18.9$ s in order to perform the 540° turn. Finally, a straight line section is driven again from $t = 28.9$ s onward. Note that for the purpose of the control strategy, the driver inputs are considered to be *a priori* unknown, and hence, the reference trailer kinematics, as described in Section III-A, are calculated in an online fashion.

B. Controller Gain Tuning

For the purpose of controller gain tuning (in particular for the gains k_1 and k_2), we analyze the transient convergence from the initial offset $\alpha(t = 0) = 0.3$ rad toward the desired alignment $\alpha_d = 0$ rad during the first phase (straight line section) of the 540° turning maneuver. Herein, we switch ON the controller at $t = 1$ s.

The controller gain settings (k_1, k_2) are tuned such that the convergence rate is maximized while ensuring that the following two additional performance criteria are met: 1) no overshoot on the articulation angle should occur and 2) the maximum absolute steering angular velocity ($\dot{\phi}_3$) may not exceed 1 rad/s in order to respect actuator saturation. Overshoot could cause dangerous situations (such as those induced by transient tail swing or rearward amplification) and increases the space required by the tractor–trailer robot in transients. Using this tuning procedure, we obtain $k_1 = k_2 = 4$ with the controller design based on feedback linearization. Furthermore, the resulting controller gain settings of the backstepping-based controller are $k_1 = 1.5$ and $k_2 = 2.5$. We note that for these parametric controller settings, the resulting closed-loop responses are almost identical for both controller types [27]. These controller gain settings will now be used in the simulations and experiments discussed in Sections V-C and VI, respectively. In Section V-C, we will also demonstrate that the additional performance requirements regarding overshoot and bounding of the actuator action are indeed satisfied for the controller tuning introduced above.

C. Simulation Results of a 540° Turning Maneuver

The effectiveness of the control strategy, with the controller design based on feedback linearization (21)–(24), is validated using simulations of the 540° turning maneuver. The results shown in Fig. 8 show that the trailer rear point indeed converges to the path of the tractor front wheel and follows the latter throughout the entire cornering maneuver, while avoiding tail swing at all times. Fig. 9 shows the response of

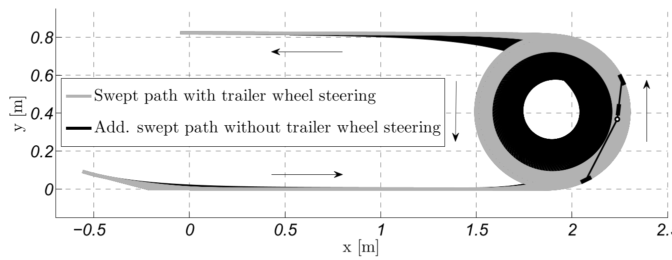

Fig. 10. Swept path for the cases with and without active trailer steering.

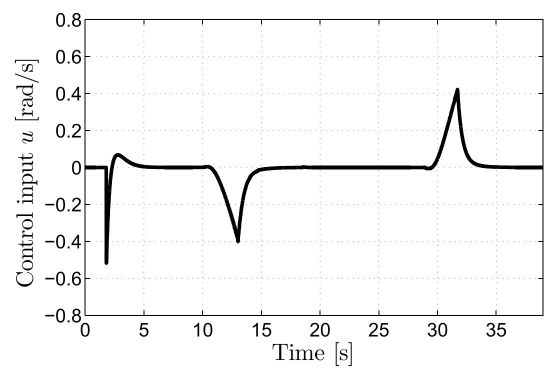

Fig. 11. Control input u (or trailer wheel angular velocity $\dot{\phi}_3$) during the 540° turning maneuver.

the tractor–trailer robot without trailer wheel steering. In both simulations, the hitch point travels the same path according to (2). Fig. 10 shows that the maximum swept path width is indeed significantly reduced using controlled trailer steering compared with the case without trailer wheel steering. In fact, a reduction of 63% in the maximum swept path width is obtained during this turning maneuver. Note that the swept path analysis is performed with the bicycle-like representation, and therefore, the width of the vehicle is not taken into account in this analysis.

Fig. 8 shows that the rear point of the trailer indeed converges toward the tractor front wheel path without causing overshoot. Moreover, Fig. 11 shows that the actuator action indeed respects the maximum bound of 1 rad/s.

This simulation study has shown that the proposed control strategy is indeed effective in simulations, and in the next section, we will validate the effectiveness of the control strategy in experiments.

VI. EXPERIMENTAL CASE STUDY

In this section, we will experimentally validate the control strategy, proposed in Section IV. Hereto, an experimental setup

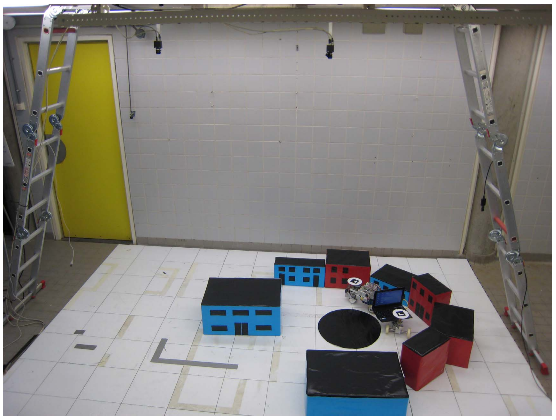

Fig. 12. Camera setup.

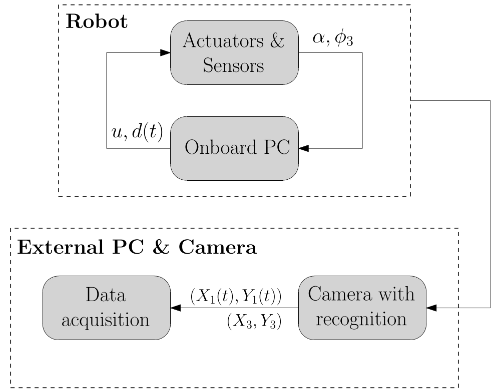

Fig. 13. Control and data acquisition architecture.

has been designed, consisting of a tractor–trailer robot and a camera setup.

1) *Tractor–Trailer Robot:* In the following, we provide a concise description of the components of the tractor–trailer robot, which are relevant from a control point of view. An extensive description of the robot design can be found in [8]. The robot is shown in Fig. 1 and consists of the following relevant components:
   a) *Actuation:* The robot is equipped with three dc motors. One of them generates the propulsion the tractor front wheel velocity $v_1(t)$ and two motors are used to steer the tractor front wheel (with angle $\phi_1(t)$) and the trailer wheel (with angle ϕ_3).
   b) *Sensing:* Each dc motor is equipped with an incremental encoder to measure: 1) the rotation of the tractor front wheel around its axis of symmetry (which can be related to the distance of the path travelled by the tractor front wheel); 2) the tractor front wheel steering angle; and 3) the trailer axle steering angle. In addition, an incremental encoder is used at the hitch point to measure the articulation angle α. Since we are using incremental encoders, inductive sensors are employed for initialization purposes.
   c) *Signal Processing and Real-Time Control:* The actuation and sensor signals are linked to a mini laptop via an EtherCAT field bus system. The mini laptop, mounted on the trailer of the robot, is used as the computational platform for the real-time implementation of the controller and to generate the inputs for the front wheel steering angle and forward velocity for the tractor front wheel (i.e., emulating the driver inputs).

   Recall that the relevant dimensions of the tractor–trailer robot are presented in Table I.

2) *Camera Setup:* We use a camera setup shown in Fig. 12 and visual recognition software, designed in [32], to measure the actual path driven by the front wheel $(X_1(t), Y_1(t))$ and the midpoint of the trailer axle $(X_3(t), Y_3(t))$.[2] These measurements will also be used to compute the path-following error d, defined as the distance between the paths of the tractor front wheel and the trailer rear point:

$$d(t) := \min_{\tau \in [0, \tau_{\max}]} \sqrt{(X_3(t) - X_1(t-\tau))^2 + (Y_3(t) - Y_1(t-\tau))^2} \tag{27}$$

for an appropriately chosen $\tau_{\max}$.

We stress that these camera measurements are used only for *a posteriori* evaluation of the performance of the active steering control strategy and are not used as feedback signals for the controller, which employs information of sensors on the robot only. Note that the computation of time difference $\hat{\tau}$ in (12) requires front wheel path and hitch point information, which both can be determined from past front wheel forward velocity and steering angle measurements only. Fig. 13 schematically shows the resulting control and data acquisition architecture. Visual markers are mounted on top of the tractor front wheel and the midpoint of the trailer axle (see Fig. 1). The positions of these markers are recognized by the two cameras covering the complete area (see Fig. 12) and an external PC processes the camera data. For demonstration purposes, an urban environment is created to define the space available for the robot to perform the turning maneuver (see Fig. 12).

A. Experimental Results

In order to validate the proposed control strategy in experiments, we consider the 540° turning maneuver, described in Section V.

The resulting measured tracking errors $\alpha - \alpha_d(t)$ and $\phi_3 - \phi_{3d}(t)$ are shown in Figs. 14 and 15, respectively. The data used for this plot are retrieved from the onboard sensors. Note that an initial offset of 0.3 rad is applied on the articulation angle α to observe the convergence toward the path driven by the tractor front wheel. A desired articulation

[2]Note that $(X_3(t), Y_3(t)) = (X_4(t), Y_4(t))$, since the trailer of the experimental robot has no overhang.

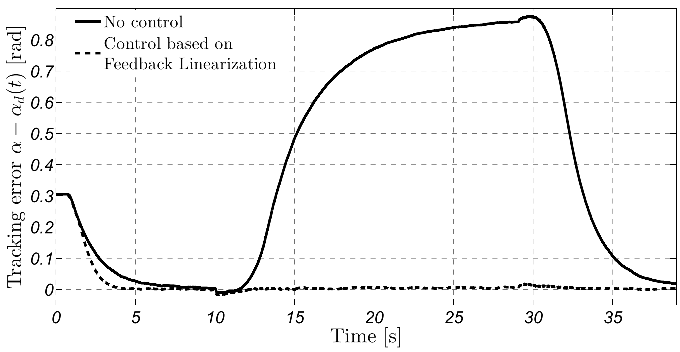

Fig. 14. Experimental tracking error $\alpha - \alpha_d(t)$.

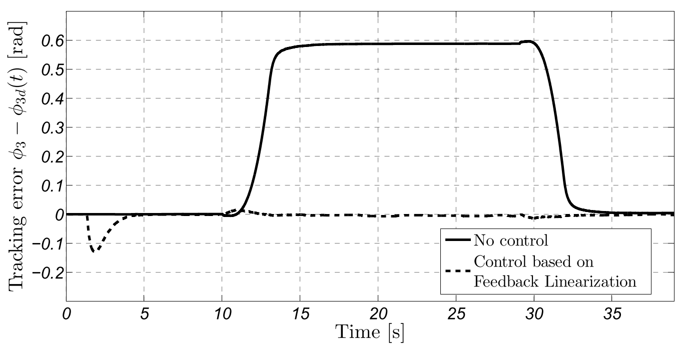

Fig. 15. Experimental tracking error $\phi_3 - \phi_{3d}(t)$.

TABLE II
RMSE VALUES OF THE TRACKING ERRORS

RMSE	No Control	Feedback Linearisation
$\alpha - \alpha_d(t)$ [rad]	0.53	0.06
$\phi_3 - \phi_{3d}(t)$ [rad]	0.40	0.02
$d(t)$ [m]	0.15	0.02

angle of $\alpha_d = 0$ rad is employed during the initial phase of the maneuver. Consequently, the tracking error $\alpha - \alpha_d$ in Fig. 14 is initially 0.3 rad. The transient error in the steering angle ϕ_3 is needed to steer the trailer toward the initially straight path.

Figs. 14 and 15 clearly show that the tracking errors converge to (a small neighborhood of) zero and that, hence, tracking is indeed achieved. It can also be observed that a large reduction in the tracking errors is attained compared with the case of an uncontrolled trailer.

Table II shows the root-mean-square error (RMSE) values of the tracking errors and the path-following error d, as defined above. Note that these values include the transient performance due to the initial offset on the articulation angle. These results in Table II confirm the large improvement in tracking performance obtained using trailer steering control.

The small remaining steady-state tracking errors are due to backlash in the drive motor, nonperfect initialization, finite sensor resolution, and unmodeled dynamical effects.

Furthermore, the data obtained with the camera setup are shown in Fig. 16. Fig. 16 shows that the trailer rear point converges to and follows the path driven by the front wheel.

The experimental results show that the proposed controller design effectively regulates the tracking errors $\alpha - \alpha_d(t)$ and $\phi_3(t) - \phi_{3d}(t)$ to (a neighborhood of) zero. Consequently, the

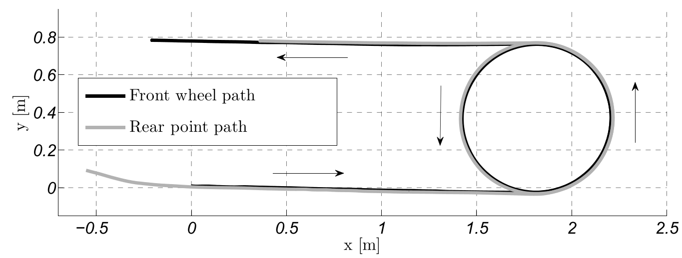

Fig. 16. Closed-loop experimental front wheel and rear point paths.

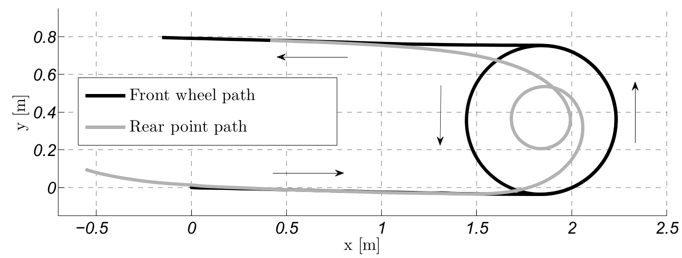

Fig. 17. Experimental front wheel and rear point paths without trailer steering.

midpoint of the trailer axle accurately follows the path driven by the front wheel and the swept path width is significantly reduced compared with the case of the unsteered trailer (see Figs. 16 and 17).

VII. CONCLUSION

A control strategy for active trailer axle steering is proposed to reduce the swept path width of a tractor–trailer robot. The control goal is formulated such that the rear point of the trailer tracks the path driven by the tractor front wheel. In this way, a significant reduction in swept path width is obtained and tail swing can be prevented. The resulting path following problem is reformulated as a state tracking problem for a kinematic model of the tractor–trailer robot. Next, controller designs based on feedback linearization and backstepping have been proposed that solve this tracking problem. The effectiveness of the proposed approach has been demonstrated in both simulation and experimental case studies.

APPENDIX A
DETAILS ON REFERENCE KINEMATICS

The controller design, as detailed in Section IV, employs the (time derivatives of the) desired trajectory $(\alpha_d(t), \phi_{3d}(t))$ (and hence those of $\phi_{4d}(t)$). Expressions for these properties of the reference kinematics will be derived in detail in this appendix.

For the derivation of the reference kinematics $(\alpha_d(t), \phi_{3d}(t))$, we use the following approach:

1) As a stepping stone, we construct a reference trajectory in terms of $\alpha_d(t), \phi_{4d}(t)$, where we recall that ϕ_4 indicates the direction of the velocity of the rear point of the trailer with respect to the trailer body (see Fig. 2).
2) Next, we convert the reference trajectory in terms of $\alpha_d(t), \phi_{4d}(t)$ to a state reference trajectory in terms of $\alpha_d(t), \phi_{3d}(t)$.

A. Reference Trajectory in Terms of $\alpha_d(t), \phi_{4d}(t)$

To construct the reference kinematics in terms of $(\alpha_d(t), \phi_{4d}(t))$, we use the feasible position $(X_1(t-\hat{\tau}(t)), Y_1(t-\hat{\tau}(t)))$ as the reference trailer rear point position $(X_{4d}(t), Y_{4d}(t))$, i.e.,

$$\begin{aligned} X_{4d}(t) &:= X_1(t-\hat{\tau}(t)) \\ Y_{4d}(t) &:= Y_1(t-\hat{\tau}(t)), \end{aligned} \tag{28}$$

where $\hat{\tau}$ is the solution of the minimization problem in (12) and (13). Furthermore, the reference heading direction $\theta_{4d}(t)$ of the rear point of the trailer is set to be equal to the orientation of the front wheel at time $t-\hat{\tau}$, i.e.,

$$\theta_{4d}(t) := \theta_1(t-\hat{\tau}(t)) \tag{29}$$

and the desired path curvature $\kappa_{4d}(t)$ of the path followed by the rear point is set to be equal to the path curvature $\kappa_1(t) := (\dot{\theta}_1(t)/v_1(t))$ of the front wheel at time $(t-\hat{\tau}(t))$:

$$\kappa_{4d}(t) := \kappa_1(t-\hat{\tau}(t)). \tag{30}$$

Then, the desired orientation $\delta_{2d}(t)$ of the reference trailer body can be expressed as follows:

$$\delta_{2d}(t) = 2\arctan\left(\frac{\Delta Y}{\sqrt{\Delta X^2+\Delta Y^2}+\Delta X}\right) \tag{31}$$

in which

$$\begin{aligned} \Delta X &:= X_2(t) - X_{4d}(t) \\ \Delta Y &:= Y_2(t) - Y_{4d}(t), \end{aligned} \tag{32}$$

where the singularity at $(\Delta X, \Delta Y) = (0,0)$ cannot occur for the solutions of (12) and (13). Using (3), the reference articulation angle $\alpha_d(t)$ can be expressed as

$$\alpha_d(t) = \delta_1(t) - \delta_{2d}(t). \tag{33}$$

Then, based on (8), the desired rear trailer point heading angle $\phi_{4d}(t)$ can be expressed as

$$\phi_{4d}(t) = \theta_{4d}(t) - \delta_{2d}(t). \tag{34}$$

The controller design, as detailed in Section IV, also employs the time derivatives of desired trajectory $(\alpha_d(t), \phi_{3d}(t))$ (and hence those of $\phi_{4d}(t)$). The expressions for these time derivatives are derived below. The time derivative of $\alpha_d(t)$ is expressed in terms of $\phi_{4d}(t)$ using (11) while substituting $(l_2, \alpha, \phi_3) = (l_2 + l_{\text{ro}}, \alpha_d(t), \phi_{4d}(t))$:

$$\dot{\alpha}_d(t) = g_1(v_1(t), \phi_1(t), \alpha_d(t), \phi_{4d}(t)) \tag{35}$$

with

$$\begin{aligned} &g_1(v_1(t), \phi_1(t), \alpha_d(t), \phi_{4d}(t)) \\ &:= \frac{1}{l_1}c_1(t) - \frac{1}{l_2+l_{\text{ro}}}c_2(t)c_{5d}(t) + \frac{l_{\text{off}}}{l_1(l_2+l_{\text{ro}})}c_1(t)c_{6d}(t) \end{aligned} \tag{36}$$

and where

$$\begin{aligned} c_{5d}(t) &:= \sin\alpha_d(t) - \cos\alpha_d(t)\tan\phi_{4d}(t) \\ c_{6d}(t) &:= \cos\alpha_d(t) + \sin\alpha_d(t)\tan\phi_{4d}(t). \end{aligned} \tag{37}$$

To avoid the singularity at $\phi_{4d} = \pm(\pi/2)$ in (37), $\phi_{4d}(t)$ is bounded to the domain $(-(\pi/2), (\pi/2))$, which is enforced by Assumption 1.1 in Section III-B.

The controller design, as detailed in Section IV, also employs other time derivatives of desired trajectory $(\alpha_d(t), \phi_{3d}(t))$, for which we need to construct the time derivative of $\phi_{4d}(t)$.

Using (33), the desired rotational velocity $\dot{\delta}_{2d}(t)$ of the trailer body can be expressed as

$$\dot{\delta}_{2d}(t) = \dot{\delta}_1(t) - \dot{\alpha}_d(t) \tag{38}$$

with $\dot{\alpha}_d(t)$ as in (35) and $\dot{\delta}_1(t) = v_1(t)\sin\phi_1(t)$ based on (1).

An expression for the time derivative of the desired heading angular velocity $\dot{\theta}_{4d}(t)$ of the trailer rear point can be constructed using (30) and the fact that $\kappa_{4d}(t) = (\dot{\theta}_{4d}(t)/v_{4d}(t))$:

$$\dot{\theta}_{4d}(t) = v_{4d}(t)\kappa_1(t-\hat{\tau}(t)), \tag{39}$$

in which the desired velocity of the rear point $v_{4d}(t)$ is calculated using angular kinematics and given by

$$v_{4d}(t) = \frac{c_2(t)\cos\alpha_d(t)}{\cos\phi_{4d}(t)} + \frac{l_{\text{off}}c_1(t)\sin\alpha_d(t)}{l_1\cos\phi_{4d}(t)}. \tag{40}$$

Then, the trailer rear point angular heading velocity $\dot{\phi}_{4d}(t)$ can be constructed using (34):

$$\dot{\phi}_{4d}(t) = \dot{\theta}_{4d}(t) - \dot{\delta}_{2d}(t), \tag{41}$$

which can be further explicated using (35), (38), and (39). Finally, using (35), the second time derivative of the desired articulation angle $\alpha_d(t)$ can be expressed as follows:

$$\begin{aligned} \ddot{\alpha}_d(t) = &\frac{\partial g_1}{\partial\phi_1(t)}\dot{\phi}_1(t) + \frac{\partial g_1}{\partial v_1(t)}\dot{v}_1(t) \\ &+ \frac{\partial g_1}{\partial\alpha_d(t)}\dot{\alpha}_d(t) + \frac{\partial g_1}{\partial\phi_{4d}(t)}\dot{\phi}_{4d}(t) \end{aligned} \tag{42}$$

with

$$\begin{aligned} \frac{\partial g_1}{\partial\phi_1(t)} &= \frac{1}{l_1}c_2(t) + \frac{1}{l_2+l_{\text{ro}}}c_1(t)c_{5d}(t) \\ &\quad + \frac{l_{\text{off}}}{l_1(l_2+l_{\text{ro}})}c_2(t)c_{6d}(t) \\ \frac{\partial g_1}{\partial v_1(t)} &= \frac{1}{l_1}\sin\phi_1(t) - \frac{1}{l_2+l_{\text{ro}}}\cos\phi_1(t)c_{5d}(t) \\ &\quad + \frac{l_{\text{off}}}{l_1(l_2+l_{\text{ro}})}\sin\phi_1(t)c_{6d}(t) \\ \frac{\partial g_1}{\partial\alpha_d(t)} &= -\frac{1}{l_2+l_{\text{ro}}}c_2(t)c_{6d}(t) - \frac{l_{\text{off}}}{l_1(l_2+l_{\text{ro}})}c_1(t)c_{5d}(t) \\ \frac{\partial g_1}{\partial\phi_{4d}(t)} &= \frac{1}{l_2+l_{\text{ro}}}c_2(t)\cos\alpha_d(t)\frac{1}{\cos^2\phi_{4d}(t)} \\ &\quad + \frac{l_{\text{off}}}{l_1(l_2+l_{\text{ro}})}c_1(t)\sin\alpha_d(t)\frac{1}{\cos^2\phi_{4d}(t)} \end{aligned} \tag{43}$$

given the expression for g_1 as in (36).

B. State Reference Trajectory $\alpha_d(t), \phi_{3d}(t)$

Here, we will convert the reference trajectory $(\alpha_d(t), \phi_{4d}(t))$ into a state reference trajectory $(\alpha_d(t), \phi_{3d}(t))$.

Let us first express $\dot{\alpha}_d(t)$ in terms of $\phi_{3d}(t)$ by substituting $(\alpha, \phi_3) = (\alpha_d(t), \phi_{3d}(t))$ in (11):

$$\dot{\alpha}_d(t) = \frac{1}{l_1}c_1(t) - \frac{1}{l_2}c_2(t)c_{3d}(t) + \frac{l_{\text{off}}}{l_1 l_2}c_1(t)c_{4d}(t), \tag{44}$$

in which

$$c_{3d}(t) := \sin\alpha_d(t) - \cos\alpha_d(t)\tan\phi_{3d}(t)$$
$$c_{4d}(t) := \cos\alpha_d(t) + \sin\alpha_d(t)\tan\phi_{3d}(t) \tag{45}$$

for $\phi_{3d} \in (-(\pi/2), (\pi/2))$ (which avoids the trailer wheel being oriented perpendicularly to the trailer body), which is enforced by Assumption 1.1 in Section III-B. Rewriting of (44) yields

$$\dot{\alpha}_d(t) = g_2(v_1(t), \phi_1(t), \alpha_d(t), \phi_{3d}(t)) \tag{46}$$

with

$$g_2(v_1(t), \phi_1(t), \alpha_d(t), \phi_{3d}(t)) := w_1(t) + w_2(t)\tan\phi_{3d}(t) \tag{47}$$

where

$$w_1(t) := \frac{1}{l_1}c_1(t) - \frac{1}{l_2}c_2(t)\sin\alpha_d(t) + \frac{l_{\text{off}}}{l_1 l_2}c_1(t)\cos\alpha_d(t)$$
$$w_2(t) := \frac{1}{l_2}c_2(t)\cos\alpha_d(t) + \frac{l_{\text{off}}}{l_1 l_2}c_1(t)\sin\alpha_d(t). \tag{48}$$

Equating (35) to (46) and solving for $\phi_{3d}(t)$ yield

$$\phi_{3d}(t) = \arctan\left(\frac{w_3(t) - w_1(t)}{w_2(t)}\right) \tag{49}$$

for $w_2(t) \neq 0$ for all t, which is enforced by Assumption 1.2 in Section III-B, and $w_3(t)$ as

$$w_3(t) := \frac{1}{l_1}c_1(t) - \frac{1}{l_2+l_{\text{ro}}}c_2(t)c_{5d}(t) + \frac{l_{\text{off}}}{l_1(l_2+l_{\text{ro}})}c_1(t)c_{6d}(t). \tag{50}$$

Using (44), the second time derivative of $\alpha_d(t)$ can now be expressed as

$$\ddot{\alpha}_d(t) = \frac{\partial g_2}{\partial\phi_1(t)}\dot{\phi}_1(t) + \frac{\partial g_2}{\partial v_1(t)}\dot{v}_1(t) + \frac{\partial g_2}{\partial\alpha_d(t)}\dot{\alpha}_d(t) + \frac{\partial g_2}{\partial\phi_{3d}(t)}\dot{\phi}_{3d}(t), \tag{51}$$

in which

$$\frac{\partial g_2}{\partial\phi_1(t)} = \frac{v_1}{l_1}\cos\phi_1(t)\left(1 + \frac{l_{\text{off}}}{l_2}c_{4d}(t)\right) + \frac{v_1}{l_2}\sin\phi_1(t)c_{3d}(t)$$
$$\frac{\partial g_2}{\partial v_1(t)} = \frac{1}{l_1}\sin\phi_1(t)\left(1 + \frac{l_{\text{off}}}{l_2}c_{4d}(t)\right) - \frac{1}{l_2}\cos\phi_1(t)c_{3d}(t)$$
$$\frac{\partial g_2}{\partial\alpha_d(t)} = -\frac{1}{l_2}c_2(t)c_{4d}(t) - \frac{l_{\text{off}}}{l_1 l_2}c_1(t)c_{3d}(t)$$
$$\frac{\partial g_2}{\partial\phi_{3d}(t)} = \frac{w_2(t)}{\cos^2\phi_{3d}(t)}. \tag{52}$$

The second time derivative of $\alpha_d(t)$ is described by both (51) and (42) and equating these expressions yields the following expression for the desired trailer wheel steering velocity $\dot{\phi}_{3d}(t)$:

$$\dot{\phi}_{3d}(t) = \left(\frac{\partial g_2}{\partial\phi_{3d}}\right)^{-1}\left(\frac{dg_1}{dt} - \frac{\partial g_2}{\partial\phi_1}\dot{\phi}_1 - \frac{\partial g_2}{\partial v_1}\dot{v}_1 - \frac{\partial g_2}{\partial\alpha_d}\dot{\alpha}_d\right) \tag{53}$$

for $w_2(t) \neq 0$ for all t.

The reference trailer kinematics are now completely described in terms of the reference state trajectory $(\alpha_d(t), \phi_{3d}(t))$ (and related time derivatives). Note that for the construction of these reference kinematics, only the information on the driver input $(v_1(t), \phi_1(t))$ and the geometries of the truck–trailers l_1, l_2, l_{off}, and l_{ro} are required.

Appendix B
Proof of Theorem 1

Consider the dynamics of the tractor–trailer robot, described by (5) and (9)–(11), and the reference trailer kinematics described in Section III-A, for which a physically feasible solution exists by the adoption of Assumptions 1 and 2. We pursue a feedback linearization approach toward stabilizing the controller design for control input $u = \phi_3$, and in doing so, we choose the following output function $h(\mathbf{x}, t) := \alpha - \alpha_d(t)$. It can be shown that the relative degree of this output equals two if

$$v_1(t)\cos\phi_1(t)\cos\alpha + v_1(t)\frac{l_{\text{off}}}{l_1}\sin\phi_1(t)\sin\alpha \neq 0. \tag{54}$$

We will address later how the satisfaction of (54) is guaranteed. Next, we employ the following time-varying coordinate transformation: $z_1 = \alpha - \alpha_d(t)$ and $z_2 = \dot{\alpha} - \dot{\alpha}_d(t)$. The system dynamics in these new coordinates with the feedback linearizing control law as in (21) and (22) yield the following linearized dynamics:

$$\dot{z}_1 = z_2$$
$$\dot{z}_2 = v. \tag{55}$$

The stabilizing control law v as in (22) then exponentially stabilizes the origin of the dynamics in (55). Note that the convergence of (z_1, z_2) to the origin implies that $(\alpha(t), \dot{\alpha}(t))$ converges to $(\alpha_d(t), \dot{\alpha}_d(t))$, and hence $\phi_3(t)$ converges to $\phi_{3d}(t)$. Therefore, the exponential stability of the origin of (z_1, z_2) implies exponential stability of the desired trajectory $(\alpha, \phi_3) = (\alpha_d(t), \phi_{3d}(t))$.

In order to avoid singularities in the control law in (21)–(24), we require that $\phi_3(t) \in (-(\pi/2), (\pi/2))$ for all $t \geq 0$ and that the condition in (54) is satisfied for all $t \geq 0$. Using the fact that $(0, 0)$ is an exponentially stable equilibrium point of the (z_1, z_2)-dynamics, we have that for any $\varepsilon_z > 0$, there exists a $\delta_z > 0$ such that $\|(z_1(t), z_2(t))^T\| \leq \varepsilon_z$ for all $t \geq 0$ if $\|(z_1(0), z_2(0))^T\| \leq \delta_z$. Now, using: 1) the continuity of the coordinate transformation to (z_1, z_2)-coordinates and 2) the continuity of the expression for ϕ_3 in terms of α and $\dot{\alpha}$

$$\phi_3 = \arctan\left(\frac{l_2\dot{\alpha} - \frac{l_2}{l_1}c_1(t) + c_2(t)\sin\alpha - \frac{l_{\text{off}}}{l_1}c_1(t)\cos\alpha}{c_2(t)\cos\alpha - \frac{l_{\text{off}}}{l_1}c_1(t)\sin\alpha}\right), \tag{56}$$

under the condition in (54), which guarantees that the denominator in (56) is nonzero, we have that for any $\varepsilon_x > 0$, there exists a $\delta_x > 0$ such that $\|(\alpha(t)-\alpha_d(t), \phi_3(t)-\phi_{3d}(t))^T\| \leq \varepsilon_x$ for all $t \geq 0$ if $\|(\alpha(0) - \alpha_d(0), \phi_3(0) - \phi_{3d}(0))^T\| \leq \delta_x$. By choosing δ_x small enough, we can ensure that Assumption 1 implies that $\phi_3(t) \in (-(\pi/2), (\pi/2))$ for all $t \geq 0$ and that Assumption 1.2 implies that indeed the condition in (54) is satisfied for all $t \geq 0$.

REFERENCES

[1] P. Fancher and C. Winkler, "Directional performance issues in evaluation and design of articulated heavy vehicles," *Vehicle Syst. Dyn., Int. J. Vehicle Mech. Mobility*, vol. 45, nos. 7–8, pp. 607–647, 2007.

[2] B. Jujnovich and D. Cebon, "Comparative performance of semi-trailer steering systems," in *Proc. 7th Int. Symp. Heavy Vehicle Weights Dimensions*, 2002, pp. 195–214.

[3] Y. Nakamura, H. Ezaki, Y. Tan, and W. Chung, "Design of steering mechanism and control of nonholonomic trailer systems," *IEEE Trans. Robot. Autom.*, vol. 17, no. 3, pp. 367–374, Jun. 2001.

[4] R. M. DeSantis, J. M. Bourgeot, J. N. Todeschi, and R. Hurteau, "Path-tracking for tractor-trailers with hitching of both the on-axle and the off-axle kind," in *Proc. IEEE Int. Symp. Intell. Control*, Oct. 2002, pp. 206–211.

[5] R. Werner, S. Mueller, and G. Kormann, "Path tracking control of tractors and steerable implements based on kinematic and dynamic modeling," in *Proc. 11th Int. Conf. Precis. Agricult.*, 2012, pp. 15–18.

[6] B. A. Jujnovich and D. Cebon, "Path-following steering control for articulated vehicles," *J. Dyn. Syst., Meas. Control*, vol. 135, no. 3, p. 031006, 2013.

[7] J. Yuan, Y. Huang, Y. Kang, and Z. Liu, "A strategy of path following control for multi-steering tractor-trailer mobile robot," in *Proc. IEEE Int. Conf. Robot. Biomimetics*, Aug. 2004, pp. 163–168.

[8] E. J. W. Roebroek, "Path following control of a tractor-steered-trailer robot," M.S. thesis, Dept. Mech. Eng., Eindhoven Univ. Technol., Eindhoven, The Netherlands, 2012.

[9] Q. Wang, M. Oya, N. Takagi, Y. Taira, and H. Ota, "Adaptive steering controller to improve handling stability for driver-combined-vehicles system," in *Proc. IEEE Int. Symp. Comput. Intell. Robot. Autom.*, Dec. 2009, pp. 409–414.

[10] D. de Bruin and P. P. J. van den Bosch, "Modelling and control of a double articulated vehicle with four steerable axles," in *Proc. IEEE Amer. Control Conf.*, vol. 5. Jun. 1999, pp. 3250–3254.

[11] Y. He and M. M. Islam, "An automated design method for active trailer steering systems of articulated heavy vehicles," *J. Mech. Design*, vol. 134, no. 4, p. 041002, 2012.

[12] S. Chang, H.-G. Xu, H.-F. Liu, and S. Chang, "Simulation on steering stability of 4WS tractor semi-trailer," in *Proc. IEEE Int. Conf. Meas. Technol. Mechatronics Autom.*, vol. 2. Apr. 2009, pp. 355–358.

[13] Q. Wang, G. Tong, and J.-M. Wu, "Adaptive lane keeping control for combination vehicles," in *Proc. Int. Conf. Comput. Sci. Artif. Intell.*, 2013.

[14] A. M. C. Odhams, R. L. Roebuck, B. A. Jujnovich, and D. Cebon, "Active steering of a tractor–semi-trailer," *Proc. Inst. Mech. Eng. D, J. Autom. Eng.*, vol. 225, no. 7, pp. 847–869, 2011.

[15] X. Ding, S. Mikaric, and Y. He, "Design of an active trailer-steering system for multi-trailer articulated heavy vehicles using real-time simulations," *Proc. Inst. Mech. Eng. D, J. Autom. Eng.*, vol. 227, no. 5, pp. 643–655, 2013.

[16] P. Fancher, C. Winkler, R. Ervin, and H. Zhang, "Using braking to control the lateral motions of full trailers," *Vehicle Syst. Dyn., Int. J. Vehicle Mech. Mobility*, vol. 29, no. S1, pp. 462–478, 1998.

[17] S. H. T. Oreh, R. Kazemi, and S. Azadi, "A new desired articulation angle for directional control of articulated vehicles," *Proc. Inst. Mech. Eng. K, J. Multi-Body Dyn.*, vol. 226, no. 4, pp. 298–314, 2012.

[18] D. de Bruin, A. A. H. Damen, A. Pogromsky, and P. P. J. van den Bosch, "Backstepping control for lateral guidance of all-wheel steered multiple articulated vehicles," in *Proc. IEEE Intell. Transp. Syst.*, Oct. 2000, pp. 95–100.

[19] G. Nitzsche, K. Robenack, S. Wagner, and S. Zipser, "Design of a nonlinear trailer steering controller," in *Proc. IEEE Intell. Vehicles Symp.*, Jun. 2014, pp. 1139–1144.

[20] A. De Luca, G. Oriolo, and C. Samson, "Feedback control of a nonholonomic car-like robot," in *Robot Motion Planning and Control*. Berlin, Germany: Springer-Verlag, 1998, pp. 171–253.

[21] K.-H. Moon, S.-H. Lee, S. Chang, J.-K. Mok, and T.-W. Park, "Method for control of steering angles for articulated vehicles using virtual rigid axles," *Int. J. Automotive Technol.*, vol. 10, no. 4, pp. 441–449, Aug. 2009.

[22] C. C. de Wit, A. D. NDoudi-Likoho, and A. Micaelli, "Nonlinear control for a train-like vehicle," *Int. J. Robot. Res.*, vol. 16, no. 3, pp. 300–319, 1997.

[23] C. Samson, "Control of chained systems application to path following and time-varying point-stabilization of mobile robots," *IEEE Trans. Autom. Control*, vol. 40, no. 1, pp. 64–77, Jan. 1995.

[24] D. Tilbury, J. P. Laumond, R. Murray, and S. Sastry, "Steering car-like systems with trailers using sinusoids," in *Proc. IEEE Int. Conf. Robot. Autom.*, May 1992, pp. 1993–1998.

[25] P. Rouchon, M. Fliess, J. Lévine, and P. Martin, "Flatness and motion planning: The car with *n* trailers," in *Proc. Int. Conf. ECC*, Groningen, Holland, 1993, pp. 1518–1522.

[26] A. Astolfi, P. Bolzern, and A. Locatelli, "Path-tracking of a tractor-trailer vehicle along rectilinear and circular paths: A Lyapunov-based approach," *IEEE Trans. Robot. Autom.*, vol. 20, no. 1, pp. 154–160, Feb. 2004.

[27] P. J. Ritzen, "Trailer steering control for an off-axle tractor-trailer robot: Reducing the swept path width," M.S. thesis, Dept. Mech. Eng., Eindhoven Univ. Technol., Eindhoven, The Netherlands, 2014.

[28] H. K. Khalil, *Nonlinear Systems*, 3rd ed. Upper Saddle River, NJ, USA: Prentice-Hall, 2002.

[29] D. M. Dawson, E. Zergeroglu, A. Behal, and W. E. Dixon, *Nonlinear Control of Wheeled Mobile Robots*. New York, NY, USA: Springer-Verlag, 2001.

[30] H. Nijmeijer and A. van der Schaft, *Nonlinear Dynamical Control Systems*. New York, NY, USA: Springer-Verlag, 1990.

[31] Z. P. Jiang and H. Nijmeijer, "Tracking control of mobile robots: A case study in backstepping," *Automatica*, vol. 33, no. 7, pp. 1393–1399, Jul. 1997.

[32] J. Caarls, "Pose estimation for mobile devices and augmented reality," Ph.D. dissertation, Dept. Mech. Eng., Delft Univ. Technol., Delft, The Netherlands, 2009.

Paul Ritzen received the B.Sc. and M.Sc. degrees in mechanical engineering from the Eindhoven University of Technology, Eindhoven, The Netherlands, in 2010 and 2014, respectively.

He is currently with Alten Nederland B.V., Eindhoven, where he is a Consultant in mechatronics.

Erik Roebroek received the M.Sc. degree in mechanical engineering from the Eindhoven University of Technology, Eindhoven, The Netherlands, in 2012.

He participated in the Nationale DenkTank (National ThinkTank) 2010, during the master's program, which aimed to increase trust in a changing society, by bridging the gap between the academic, public, and private sectors in The Netherlands. After an academic internship with the University of Waterloo, Waterloo, ON, Canada, he became a Project Manager with Vanderlande, Veghel, The Netherlands, mainly focusing on international baggage handling system projects and internal improvements.

Nathan van de Wouw (M'09) was born in 1970. He received the M.Sc. (Hons.) degree and the Ph.D. degree in mechanical engineering from the Eindhoven University of Technology, Eindhoven, The Netherlands, in 1994 and 1999, respectively.

He was with Philips Applied Technologies, Eindhoven, in 2000. In 2001, he was with the Netherlands Organisation for Applied Scientific Research, Delft, The Netherlands. He was a Visiting Professor with the University of California at Santa Barbara, Santa Barbara, CA, USA, in 2006/2007, the University of Melbourne, Melbourne, VIC, Australia, in 2009/2010, and the University of Minnesota, Minneapolis, MN, USA, in 2012 and 2013. He is currently a Full Professor with the Mechanical Engineering Department, Eindhoven University of Technology, The Netherlands, an Adjunct Full Professor with the University of Minnesota, U.S.A. and a part-time Full Professor with the Delft Center for Systems and Control at the Delft University of Technology, The Netherlands. He has authored a large number of journal and conference papers and the books entitled *Uniform Output Regulation of Nonlinear Systems: A Convergent Dynamics Approach* (Birkhauser, 2005) with A. V. Pavlov and H. Nijmeijer and *Stability and Convergence of Mechanical Systems with Unilateral Constraints* (Springer-Verlag, 2008) with R. I. Leine. His current research interests include the analysis and control of nonlinear/hybrid systems, with applications to vehicular platooning, high-tech systems, resource exploration, smart energy systems, and networked control systems.

Prof. van de Wouw is an Associate Editor of *Automatica* and the IEEE TRANSACTIONS ON CONTROL SYSTEMS TECHNOLOGY journals.

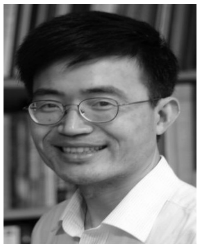

Zhong-Ping Jiang (M'94–SM'02–F'08) received the M.Sc. degree in statistics from the University of Paris XI, Paris, France, in 1989, and the Ph.D. degree in automatic control and mathematics from the Ecole des Mines de Paris, Paris, in 1993.

He is currently a Professor of Electrical and Computer Engineering with the Tandon School of Engineering, New York University, Brooklyn, NY, USA. He has co-authored the books entitled *Stability and Stabilization of Nonlinear Systems* (Springer, 2011) with Dr. I. Karafyllis and *Nonlinear Control of Dynamic Networks* (Taylor & Francis, 2014) with Dr. T. Liu and Dr. D. J. Hill. His current research interests include stability theory, robust/adaptive/distributed nonlinear control, adaptive dynamic programming, and their applications to information, mechanical, and biological systems.

Prof. Jiang is a fellow of the International Federation of Accountants. He is the Deputy Co-Editor-in-Chief of the *Journal of Control and Decision* and has served as an Associate Editor for several journals.

Henk Nijmeijer (F'00) was born in 1955. He received the M.Sc. and Ph.D. degrees in mathematics from the University of Groningen, Groningen, The Netherlands, in 1979 and 1983, respectively.

He was with the Department of Applied Mathematics, University of Twente, Enschede, The Netherlands, from 1983 to 2000. Since 1997, he has been with the Department of Mechanical Engineering, Eindhoven University of Technology, Eindhoven, The Netherlands, where he has been a Full Professor and the Chair of the Dynamics and Control Group since 2000. He is currently the Scientific Director of the Dutch Institute of Systems and Control Graduate School. He has authored a large number of journal and conference papers, and several books. His current research interests include the broad scope of dynamics and control and their applications.

Prof. Nijmeijer has been an International Federation of Accountants Council Member since 2011. He was awarded in the IEE Heaviside Premium in 1990. He has been an Honorary Knight of the Golden Feedback Loop Norwegian University of Science and Technology (NTNU) since 2011. He was the Editor-in-Chief of the *Journal of Applied Mathematics* until 2009, a Corresponding Editor of the *SIAM Journal on Control and Optimization*, and a Board Member of the *International Journal of Control*, *Automatica*, the *Journal of Dynamical Control Systems*, the *International Journal of Bifurcation and Chaos*, the *International Journal of Robust and Nonlinear Control*, the *Journal of Nonlinear Dynamics*, the *Journal of Applied Mathematics and Computer Science*, and *Hybrid Systems*. He is an Editor of *Communications in Nonlinear Science and Numerical Simulations*.